U-0698
0210-L
N83-84(02-17)-L

ILLINOIS POWER COMPANY

CLINTON POWER STATION, P.O. BOX 678, CLINTON, ILLINOIS 61727

February 17, 1984

Docket No. 50-461

Director of Nuclear Reactor Regulation
Attention: Mr. A. Schwencer, Chief
Licensing Branch No. 2
Division of Licensing
U. S. Nuclear Regulatory Commission
Washington, D. C. 20555

Subject: Clinton Power Station Unit 1
SER Issues - Pool Dynamics
Outstanding #9/Confirmatory #13

Dear Mr. Schwencer:

Your letter of November 14, 1983 requested additional information relative to suppression pool dynamic concerns as applicable to the Clinton Power Station (CPS). Enclosed are CPS responses for the NRC Staff review. Included are responses to Mechanical Engineering Branch questions numbers 210.01, 210.02, 210,03, 210.04 and Containment System Branch questions 480.27 and 480.28. We believe that these responses will resolve the particular concerns and close out SER Outstanding Issue #9 and Confirmatory Issue #13.

Sincerely yours,

J. D. Geier
Manager
Nuclear Station Engineering

GEW/lam

Enclosure

cc: G. A. Harrison, NRC Clinton Licensing Project Manager
L. C. Ruth, NRC CSB
D. Terao, NRC MEB
NRC Resident Office
Illinois Department of Nuclear Safety

A001
1/1

NRC QUESTION NO. 210.01

In a comparison of the quencher and support per NUREG-0763, you have shown that the quencher base support is welded to the basemat and is provided with rigid supports from the SRV discharge line to the drywell wall. It is not clear whether the rigid supports are welded directly to the SRV pipe or to a collar around the pipe. In the staff's opinion, if the supports are welded directly to the SRV pipe, the welded attachment could cause excessive localized bending stresses and potentially harmful thermal gradients in the piping following actuations of the safety-relief valves. Furthermore, the large number of stress cycles could result in fatigue failure in the piping. Provide the quencher support details and the results of your stress analyses for the SRV piping at the support attachment. Provide assurance that the structural integrity of the piping and the quencher support capabilities are not compromised.

RESPONSE

Each of the 16 SRV discharge lines is rigidly restrained to the drywell wall by a support connected immediately above the quencher inlet. This support consists of collar-type attachment welded to the piping, as shown in Figure 210.01-1. As per Code Subsection ND requirements, localized bending stresses due to mechanical and thermal expansion loading have been considered for the piping at the attachment location. As shown in Table 210.01-1, an envelope of finite element analyses of these connections has been generated. The local stresses from the attachments were added to the pipes' nominal bending and pressure stresses. A summary of maximum pipe stresses is shown in Table 210.01-1.

Fatigue concerns for SRV discharge piping were raised by the NRC for BWR Mark I and Mark II plants. Generic programs have addressed these concerns,

and have shown acceptable fatigue results. Mark II fatigue results were reviewed with the ACRS on August 7, 1981. The primary fatigue concern was for the portion of the SRV piping in the wetwell airspace, where a fatigue crack could result in steam bypassing the suppression pool. This concern does not apply to the location in question on the Clinton SRV piping, which is submerged in the pool. Also, due to the use of a low-low setpoint logic, the number of design SRV actuations (hence thermal and mechanical load cycles) for Clinton typically will be lower than for Mark I's and Mark II's.

As shown in Table 210.01-1, there is a large margin for Equation 10 and 11 stresses. Although not required, thermal gradient stresses if added to Equations 10 and 11 would not create a fatigue problem. Also, a higher allowable stress for these equations could be justified per Code Case N-318, since the number of stress cycles would be less than 7000.

Therefore, per paragraph ND-3645 of the Code, these attachments to the SRV piping were conservatively designed and are well within ND-3650 stress allowables.

Figure 1 - SRV Discharge Line Support - Welded Attachment Detail

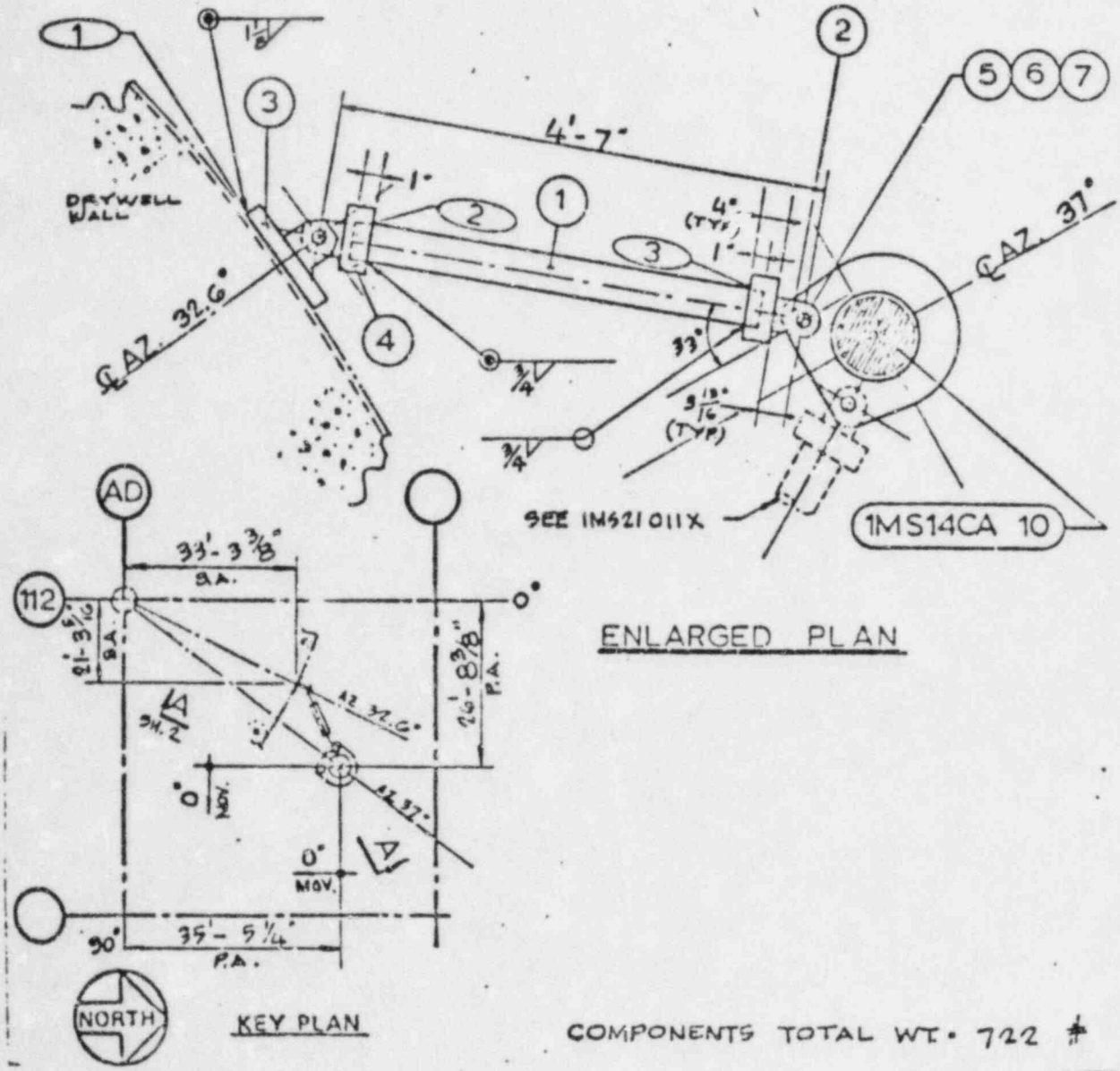

Sheet 1 of 4

Figure 1 - SRV Discharge Line Support - Welded Attachment Detail

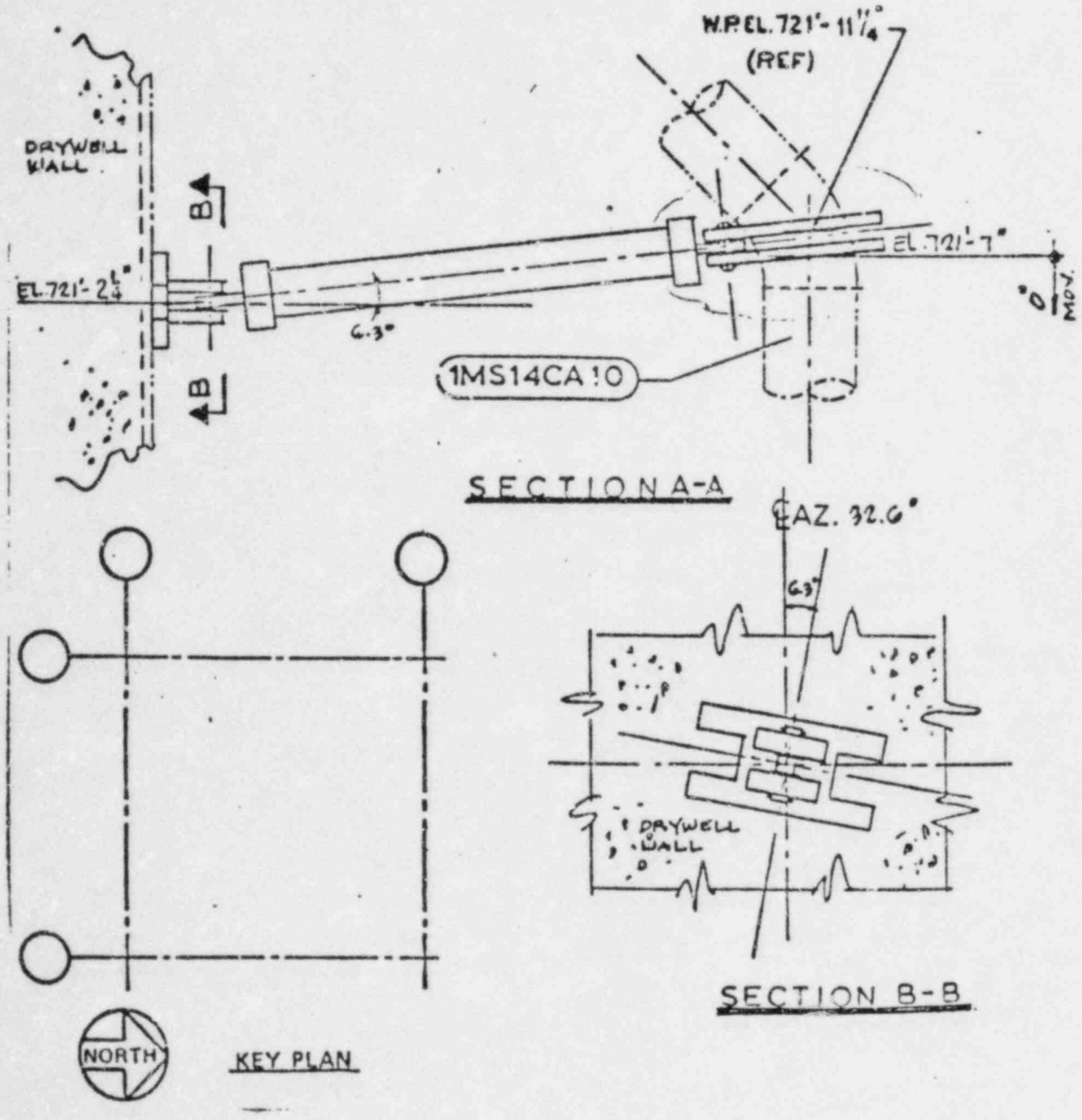

Sheet 2 of 4

Figure 1 - SRV Discharge Line Support - [illegible]d Attachment Detail

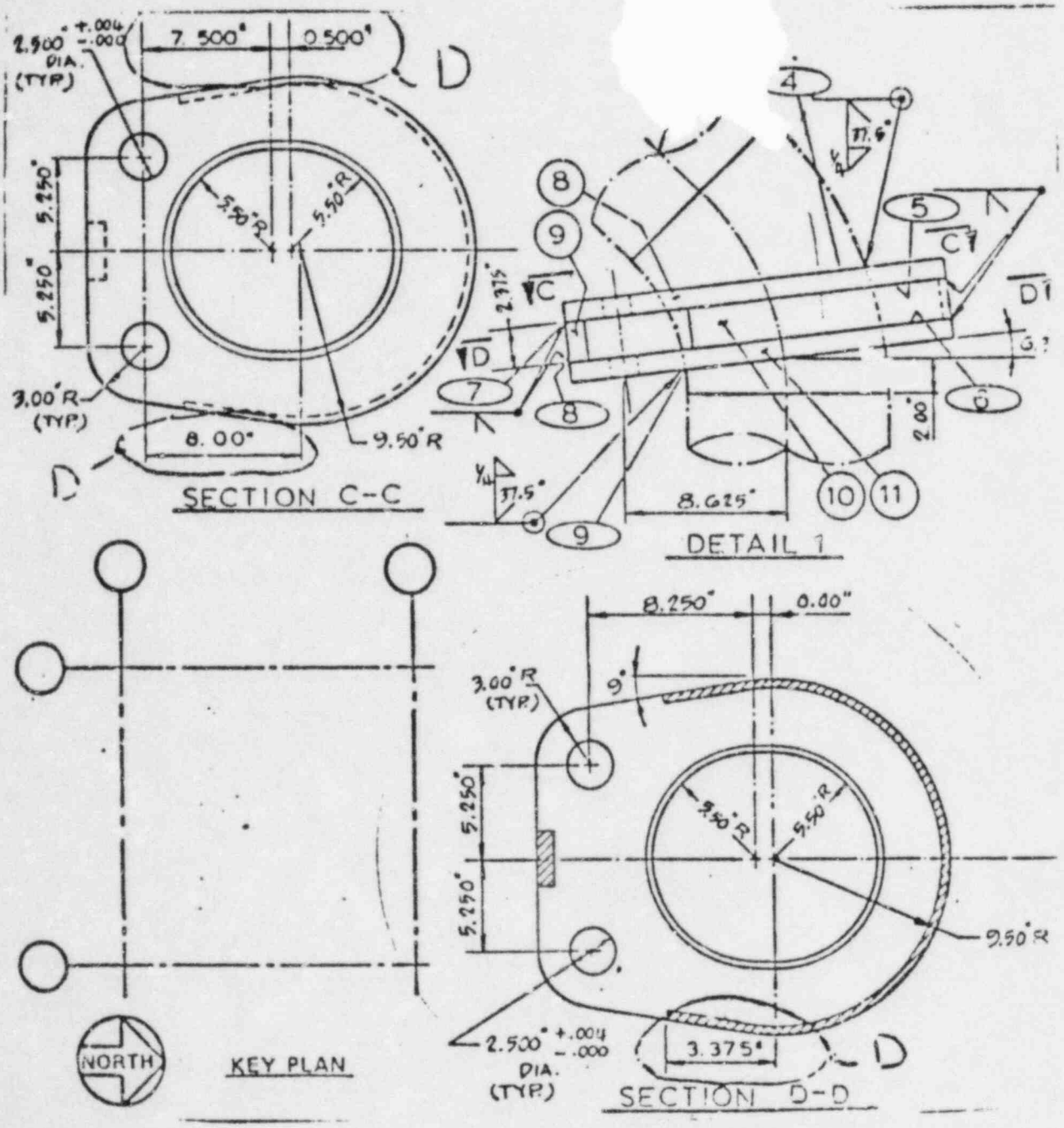

Sheet 3 of 4

Figure 1 - SRV Discharge Line Support - Welded Attachment Detail

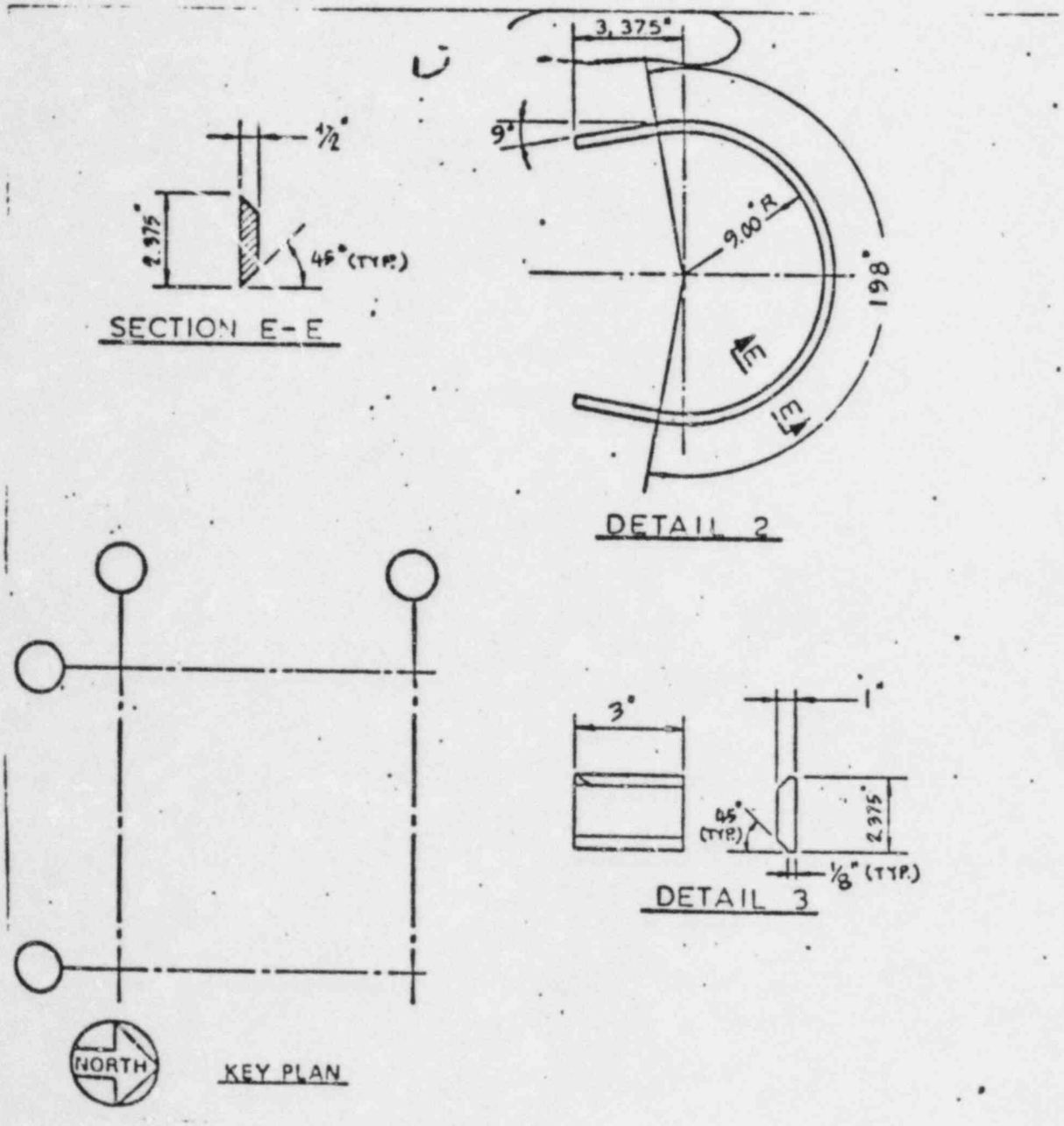

Sheet 4 of 4

TABLE 210.01-1

MAXIMUM STRESS SUMMARY
SRV DISCHARGE LINE AT SUPPORT
WELDED ATTACHMENT LOCATION

Code Equation (ND-3652)	Allowable Stress (psi)	Calculated Stress (psi)
9	19,080	13,535
10	27,475	10,400
11	43,375	12,900

Notes:

1) Calculated stresses represent an envelope of all 16 SRV discharge lines, and include the effects of both local attachment stress and nominal pipe stress.

2) Equation 9 allowable stress is for Service Level B - corresponding calculated stress conservatively envelopes Service Levels B, C and D.

3) Equation 10 and 11 calculated stresses conservatively include attachment local stress due to both thermal expansion and mechanical loads.

NRC QUESTION NO. 210.02

The quencher device is classified as an ASME Code Class 3 component. Provide the basis for assuring that the quencher device has been adequately designed for all applicabie stresses resulting from the actuation of the safety-relief valves including localized bending stresses and thermal gradients.

RESPONSE

General Electric Company analyzed four critical locations (shown on Figure 1 of Attachment 210.02) on the X-Quencher in order to assure that the quencher device meets the requirements of Subsection NB-3600 of ASME Code.

The analysis confirmed that the X-Quencher has been adequately designed to withstand all normal and upset condition loads including localized bending stresses and thermal gradients. See Attachment 210.02 for the General Electric Company "Report on NRC Question About Thermal Gradient Stresses for Clinton X-Quencher".

Attachment 210.02

To: G. E. Wuller
P. E. Walberg

P.E. Walberg

GENERAL ELECTRIC COMPANY

LICENSING ACTION NOTICE

CLINTON I

1/6

Notice No. 45 Rev. 0

Transmittal Date: January 16, 1984

Responds to: IPC Request dated 12/08/84

SUBJECT: Thermal Gradient Stesses for Clinton X-quencher

FSAR: N/A

NRC QUESTION NO. 210.02

ACTION REQUIRED:

See attached memo

Submitted by _____ (Licensing Engineer) Date 1/16/84

Reviewed by _____ (Project Engineer) Date 1/16/84

Approved by _____ FOR F.P. Downey (Project Manager) Date 1/16/84

2/6

GENERAL ELECTRIC CO.
SAN JOSE, CALIFORNIA
PLANT PIPING DESIGN
DESIGN MEMO #1Z3-8402
DESIGN RECORD FILE DRF NO. B21-00042

VERIFICATION CONTAINED IN DRF

REPORT ON NRC QUESTION ABOUT THERMAL GRADIENT STRESSES FOR CLINTON X-QUENCHER

PREPARED BY: A. K. Dhawan

A. K. Dhawan, Engineer
Plant Piping Design

REVIEWED BY: H. L. Hwang

H. L. Hwang, Principal Engineer
Plant Dynamic Methods & Applications

REVIEWED BY: H. M. Srivastava 1/13/84

H. M. Srivastava, Principal Engineer
Plant Piping Design

APPROVED BY: J. C. Atwell 1/13/84

J. C. Atwell, Manager
Plant Piping Design

JANUARY 1984

1.0 INTRODUCTION.

Clinton X-Quencher had been analyzed according to the requirements of the Subsection NB-3600 of the ASME Code, Section III. The NRC had expressed some concern about the fatigue life of the X-Quencher due to thermal gradient and local bending stresses. Although NB-3600 does not require a detailed fatigue evaluation (and the intent of NB-3600 had been met in the previous analysis), it was decided to reanalyze four critical locations (shown on Figure #1) on the X-Quencher to the requirements of Subsection NB-3600 of ASME Code to alleviate NRC's concern on the subject. The analysis consisted of calculating the fatigue usage factor at these locations for 40 years of the plant life.

2.0 LOADS AND METHOD.

The four locations (designated as 'A', 'B', 'C' and 'D') represent the critical sections. Location 'A' is the SRV piping - quencher interface point and was selected because it is a dissimilar metal connection. Location 'B' is the X-Quencher adapter - reducer interface connection. Location 'C' is the quencher arm - body interface connection and location 'D' is the quencher connection to the pedestal adaptor. Fatigue usage factor was calculated for these locations using peak stress 'S_p' and alternating stress 'S_a' obtained from Equations 11 and 14 of Subsection NB-3600 respectively. To calculate the worst thermal gradients across these sections, the most severe transient was used. The transient consists of a step change from 70°F to 350°F. Appropriate heat transfer coefficients were calculated and applied for the transient. The stresses due to these thermal gradients were combined with the stresses due to the moment loading at these locations and the pressure stress. Secondary stress indices C_1, C_2 and C_3 and local stress indices K_1, K_2 and K_3 were calculated and applied for these locations based on their configurations.

A finite element model was made for location 'D' because of its complex geometric configuration and the consequent difficulty in calculating stress indices. Peak stress was calculated using this model for the same thermal transient, the moment loading and the pressure loading.

3.0 RESULTS AND CONCLUSIONS.

The fatigue usage factors calculated are shown in Table #1.

TABLE 1

LOCATION	USAGE FACTOR
'A' SRV PIPING SIDE	0.84
'A' QUENCHER SIDE	0.32
B	0.21
C	0.53
D	0.01

The thermal gradients calculated are shown in Table #2.

TABLE 2

LOCATION	ΔT_1*	ΔT_2*	T_A*	T_B*	TIME** MINUTES
A	120.838	126.180	94.956	109.951	0.010
B	52.430	183.841	79.405	79.405	0.020
C	118.026	97.114	95.083	154.196	0.240
D	By Finite Element Analysis.				

* Refer to Subsection NB-3600 for definition.
** The time which creates maximum combined stresses.

Since the usage factors for the four critical sections are less than 1.0, we can safely conclude that the Clinton X-Quencher can withstand all normal and upset condition loads including the stresses due to thermal gradient and local bending effects.

4.0 REFERENCES.

(1) ASME Boiler and Pressure Vessel Code Section III - 1983 Edition.

(2) DRF #B21-42, X-Quencher, Pedestal Mounted.

(3) Stress Report Data Sheet for X-Quencher #22A5408AB.

(4) Design Specification for Quencher X-Type #21A2139.

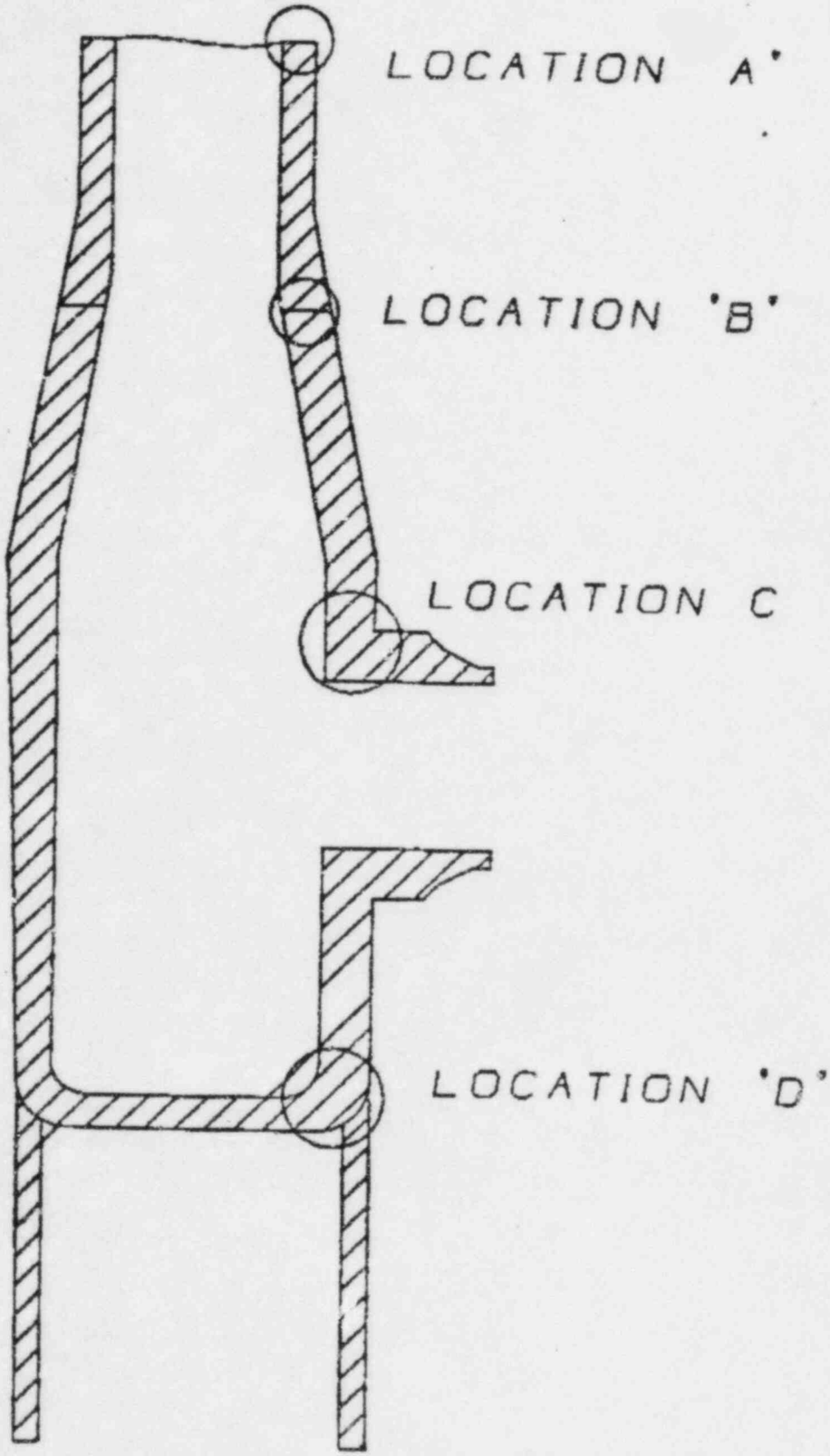

5/6

CLINTON X-QUENCHER CRITICAL LOCATIONS

FIGURE #1

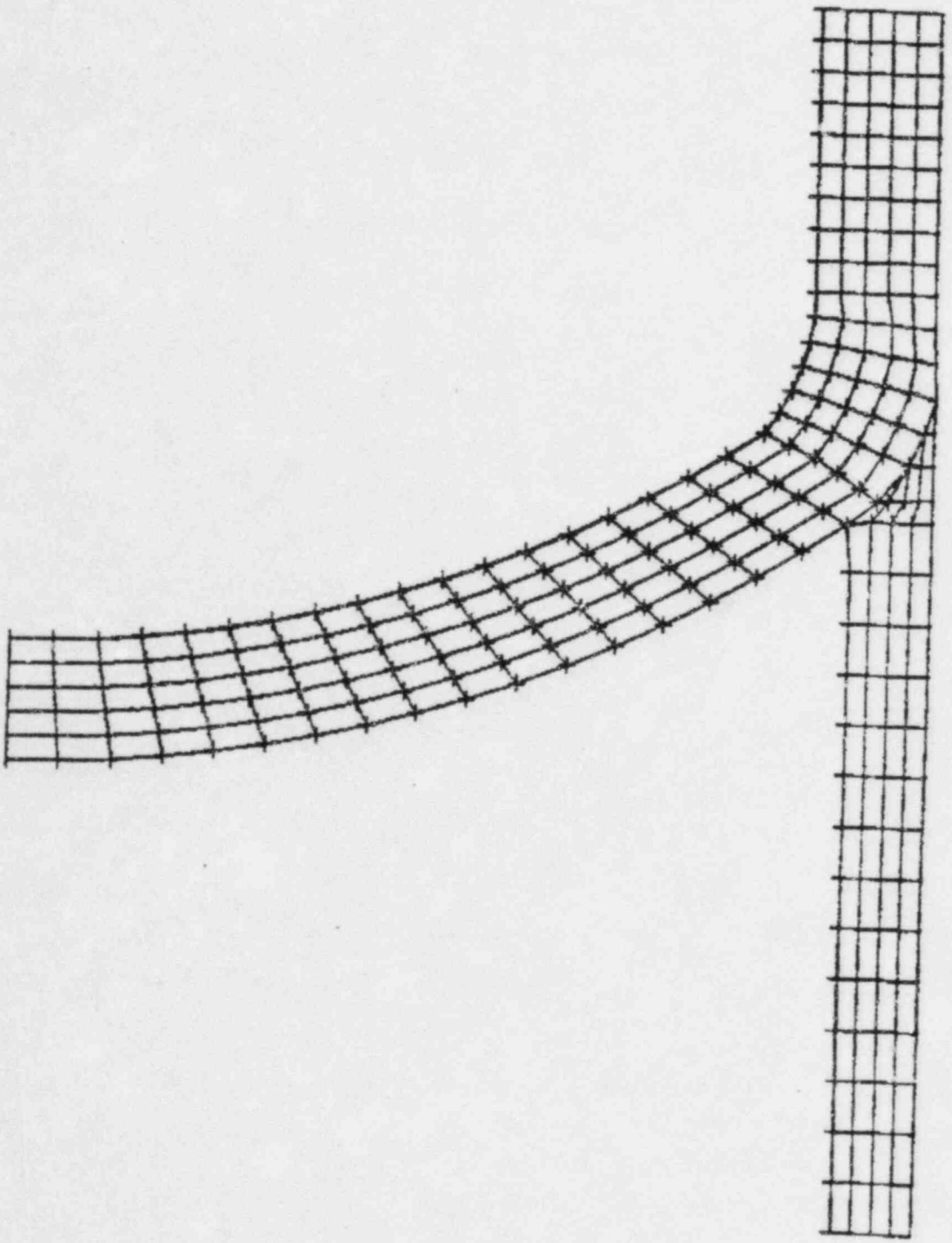

FIGURE #2

FINITE ELEMENT MODEL OF LOCATION 'D'

NRC QUESTION NO. 210.03

The staff has been informed that several piping systems inside the suppression pool wetwell area which are subjected to pool swell impact and drag loadings are restrained using linear (vertical) pipe supports with pinned-pinned end connections. Provide the basis for assuring that the design of these piping systems have properly considered the lateral instability of those pipe supports with pinned-pinned end connections when subjected to the non-cyclic compressive loadings as experienced during a pool swell event.

RESPONSE

For pool swell loading, Clinton piping systems above the suppression pool are typically restrained in the vertical direction utilizing pinned-pinned rigid supports. The concern is related to lateral instability of piping systems under steady-state pool swell/froth drag loading. A review was made of all affected piping systems with significant runs of horizontal piping. This review has shown that the affected piping is rigidly restrained in the lateral direction for seismic/pool dynamic response spectrum loading. The lateral rigid restraints are adequately designed and spaced to eliminate potential instability problems. The NRC concern has therefore been considered in the Clinton design.

NRC QUESTION NO. 210.04

The staff has been informed that the response spectrum method of analysis is used in the design of the control rod drive (CRD) piping for LOCA-related loads. Furthermore, we were informed that the CRD piping analyses is performed by Reactor Controls, Inc. (RCI). In accordance with SRP Section 3.9.1, provide a description of the computer program used by RCI in the CRD piping analysis including the extent and limitations of its application and the method of verification.

RESPONSE

RCI used four computer programs in the CRD piping analysis. The four programs were TPIPE Version 5.1, EASE 2 Version 13.4, E2A17 Version 13.4B, and EWELD Version 2.0. The description of each computer program including the extent of its application and the method of verification is shown on attachments 210.04-1 to 210.04-4.

ATTACHMENT 210.04-1

COMPUTER PROGRAM: TPIPE Version 5.1 Dated 6/23/83

AUTHORS: PMB Systems Engineering
San Francisco, CA.

DESCRIPTION:

A special purpose computer program using finite element scheme to perform static and dynamic linear elastic analyses of power related piping system. Dynamic analysis options include:

1. Frequency Extraction
2. Response Spectrum
3. Time History Modal Superposition
4. Time History Direct Integration

ADDITIONAL CAPABILITIES INCLUDE:

1. Plot undeformed and deformed geometry.
2. Post process pipe member end forces through ASME Section III Class 1, 2, or 3 Stress Evaluation Equations, and provide support load and pipe attachment evaluation.
3. Thermal transient heat analysis to provide linear thermal gradient, T1 nonlinear thermal gradient, T2, and gross discontinuity expansion difference.

The major computational algorithms which solve the linear equilibrium equations and calculate the dynamic structural frequencies and mode shapes were taken from the efficient General Purpose Structural Analysis Program SAPIV.

EXTENT OF APPLICATION:

TPIPE has been utilized to perform the following category of design analysis for the CRD Hydraulic System piping.

1. Static
2. Frequency Analysis
3. Response Spectrum
4. Time History Direct Integration
5. ASME Class II and B31.1 Code Evaluation

VERIFICATION:

The verification for the program has been done by PMB Systems Engineering. A total of thirty-six (36) test cases were utilized. Portions of the program are compared with hand calculations. The dynamic analysis was compared with results from accepted computer programs.

In addition the seven (7) NRC Benchmarks referred within Item II.2 or C.(5) in SRP 3.9.1 NUREG-0800 have been executed through TPIPE.

REFERENCED COMPUTER PROGRAMS:

PISOL	--	EDS Nuclear
NUPIPE	--	Control Data Corp.
STARDYNE	--	Control Data Corp.
SAP IV	--	Control Data Corp.

ATTACHMENT 210.04-2

COMPUTER PROGRAM: EASE2 Version 13.4 Dated 4/10/82

AUTHORS: Engineering Analysis Corporation
Berkeley, CA.

SOURCE: Control Data Cybernet Services
Sunnyvale, CA.

PROGRAM DESCRIPTION:

EASE2 is a general purpose computer program that uses finite element scheme to analyze linear elastic static and dynamic models. The element library consists of beams, pipe, isoparametric solids, isoparametric 2-D elements, shell, plate and membrane. EASE2 is capable of performing the following analyses.

1. Static
2. Eigenvalue
3. Mode Superposition
4. Direct Integration
5. Response Spectrum

EASE2 employs a modified Gauss elimination procedure in banded equation block solver for static analysis. The static analysis model (K-Matrix) is fully compatible with the dynamic analysis method.

EXTENT OF APPLICATION:

EASE2 has been utilized at RCI for the design analysis of finite element models of support structures for the CRD piping. The options used are

1. Static
2. Eigenvalue Extraction
3. Direct Integration
4. Response Spectrum

VERIFICATION:

The EASE2 has a substantial user base. This program has been used by various nuclear engineering facilities. EASE2 has been verified by its authors. The test cases are published as the EASE2 Example Problems Manual by Fred Peterson Engineering Analysis Corporation.

Specifically the program was verified in the following three ways.

1. Theoretical results published in text books.
2. Numerical results produced by other previously verified computer programs.
3. Hand calculations.

EXTENDED COMPUTER PROGRAMS:

1.	SAP IV	University of California, Berkeley
2.	ANSYS	Swanson Analysis Systems Inc., Elizabeth, PA.

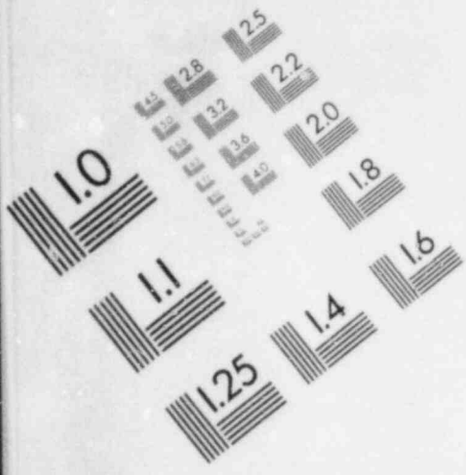

IMAGE EVALUATION TEST TARGET (MT-3)

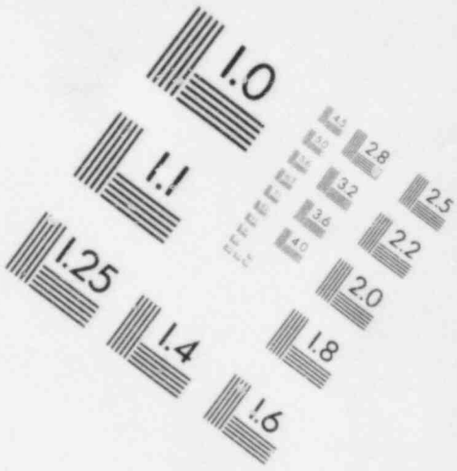

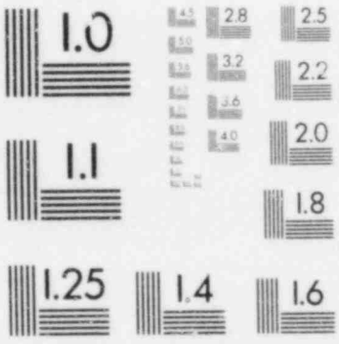

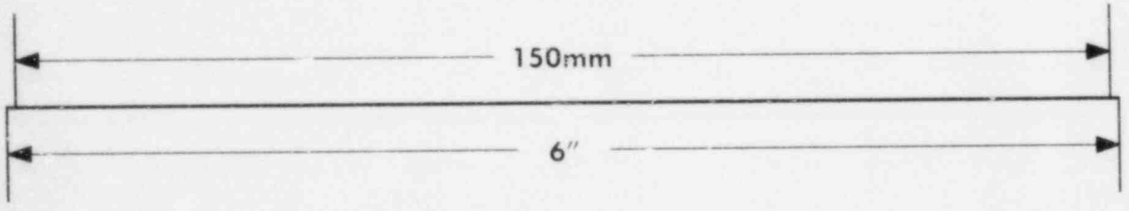

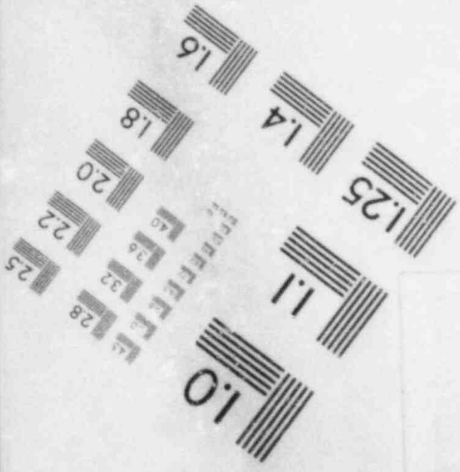

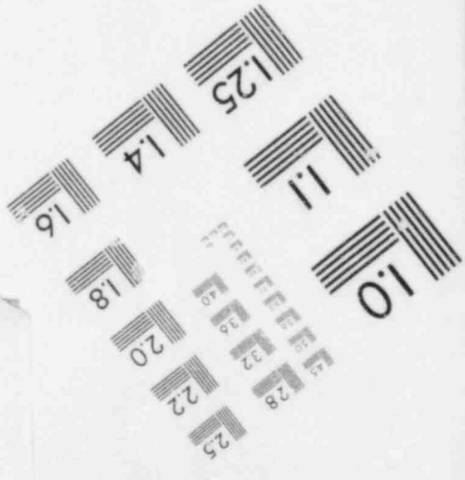

ATTACHMENT 210.04-3

COMPUTER PROGRAM: E2A17 Version 13.4B Dated 8/22/83

AUTHORS: Engineering Analysis Corporation
Berkeley, CA.

DESCRIPTION:

E2A17 is a post processing program that uses the geometry and end forces and moments from the EASE2 program and performs steel design check calculations according to the provisions of Section III Nuclear Power Plant Requirements ASME Boiler and Pressure Vessel Code, Article XVII-2000, Linear Elastic Analysis, 1977 (1979 Winter Addenda).

EXTENT OF APPLICATION:

E2A17 is utilized in evaluating results provided by "EASE2" in the analysis of support structures for the CRD piping.

VERIFICATION:

E2A17 has been verified against hand calculations.

ATTACHMENT 210.04-4

COMPUTER PROGRAM: EWELD Version 2.0 Dated 10/03/83

AUTHORS: Ramji Chaudhari, Simon Schmukler and Kent Johnson

PROGRAM DESCRIPTION:

EWELD is a post-processing program that uses the forces and moments at element end-nodes and the section properties data to calculate fillet weld thickness, lamellar tearing and flare bevel weld sizes.

EXTENT OF APPLICATION:

EWELD is utilized as a post-processor to the E2A17 computer programs, to analyze weld size and tabulate reactions as a step in the design analysis of CRD piping support structures.

VERIFICATION:

EWELD program has been verified against hand calculations.

NRC QUESTION NO. 480.27

In order to demonstrate the adequacy of the Clinton containment design regarding LOCA-related hydrodynamic loads, the following information needs to be supplied for our review.

1) Show by comparison of design and plant parameters the applicability of using the GESSAR-II generic load definitions (as modified by Appendix C of proposed NUREG-0978) for Clinton. Include a discussion of the plant design differences between Clinton and GESSAR-II that could make the hydrodynamic loads higher for the Clinton design, (e.g., HCU floor open area less than 25%, gratings above the weir wall or within 19 feet of the suppression pools initial surface).

RESPONSE

Table 480.27-1 gives a comparison of the plant design parameters for the GESSAR-II 238 Standard containment and the Clinton containment. A review of these data show that the Clinton plant has a 218 size drywell in a 238 size containment. This results in the containment and suppression pool volumes being relatively larger in the Clinton plant than in the Standard 238 plant. These larger volumes translate directly into more capacity to absorb energy during accident events. Thus, there is no need to change the design basis load definition to assure a conservative design.

The geometry of the horizontal vent system is a primary determinant of the LOCA-related hydrodynamic loads. Table 480.27-1 shows that these systems are similar for the two plants, except Clinton has fewer vents. This smaller number of vents has been considered in design basis calculations and has resulted in no need to alter the generic LOCA design parameters for the Clinton plant.

Clinton has some unique features which do not occur in the standard plant design. These include a grating floor located

approximately 5 feet above the normal suppression pool surface, a cantilevered HCU floor, and a grating floor that is supported from the weir wall and extends over the weir annulus.

The concrete portion of the HCU floor constitutes some 31% of the annular area between the drywell and the containment. The remainder of the structure (69% of the open area) at this level is comprised of grating and open areas. The total open area at the 755'0" elevation is greater than 26%, therefore, the GESSAR load definition is applicable to Clinton. The weir annulus is covered by a grating floor. This deviation from the standard plant design and the determination of the design loads are discussed in the response to Question 480.27-2. The load definition for the grating floor located at approximately 5 feet above the normal suppression pool surface is also discussed in response to Question 480.27-2.

TABLE 480.27-1

COMPARISON OF PLANT DESIGN PARAMETERS

Parameter	GESSAR-II		CLINTON	
	Drywell	Containment	Drywell	Containment
Outside diameter (ft)	83.0	120.5	79.0	130.0
Inside diameter (ft)	73.0	120.0	69.0	124.0
Net free Volume (ft^3)	274,960	$1.14X10^6$	246,500	$1.55X10^6$
Suppression Pool Surface Area (ft^2)	482	5900	455	7175
Suppression Pool Depth (ft)				
- Low Water Level	19.92	19.92	18.92	18.92
- High Water Level	20.42	20.42	19.42	19.42
Suppression Pool Volume - HWL (ft^3)	12,315	120,460	10,930	139,300
Horizontal Vents				
- Number	120	N/A	102	N/A
- Diameter (in)	27.5	N/A	27.5	N/A
- Total Area (ft^2)	495	N/A	420	N/A
- Submergence T/M/B (ft)	7.0/11.5/16.0	N/A	7.0/11.5/16/0	N/A
Weir Annulus				
- Outside diameter (ft)	69.0	N/A	69.0	N/A
- Inside diameter (ft)	64.7	N/A	64.7	N/A
- Height (ft)	26.08	N/A	23.75	N/A

NRC QUESTION NO. 480.27

In order to demonstrate the adequacy of the Clinton containment design regarding LOCA-related hydrodynamic loads, the following information needs to be supplied for our review.

2) Provide and justify the load definitions used for structures and equipment that are beyond the scope of the generic load envelope contained in GESSAR-II (e.g., pipes within 0.25 feet of the top of the weir wall, submerged structures in the path of the horizontal vent water jets, and structures in the bulk pool region less than 4 feet long and/or closer than 6 feet from the initial pool surface).

RESPONSE

Structural steel, piping, pipe supports, conduit and other components in the drywell are subject to the weir swell loading. A definition of this load is given in Section 3B.5.1.5 of GESSAR-II. This load definition is the result of bounding static analyses performed for the spectrum of Mark III containment parameters. Clinton specific parameters were used in the GESSAR-II models to generate time dependent load definitions. The details of this load definition are included in the attached material.

The structural steel, piping, pipe supports, conduit, and other components affected by the weir swell loads have been assessed for the loads described in the attached material.

Essential components (those components required to function during safe shutdown) have been assessed to ensure that they remain functional during the weir swell phenomona. Non-essential components have been assessed to ensure that they will remain in place during and following this event. The structural steel supporting essential components has been assessed to the criteria given in Section 3.8 of the FSAR. The steel supporting

non-essential components has been assessed to assure that it will remain in place.

The only submerged structures in the path of the horizontal vent water jets are the quenchers, whose design is discussed in Section 3BA.7 of GESSAR-II.

The load definition for the structural steel and piping within 6 feet of the initial pool surface and/or less than four feet in length is based on the acceptance criteria in Appendix C of proposed NUREG-0978.

ATTACHMENT 480.27-2

INTRODUCTION

The purpose of this material is to describe the development and to discuss the models used to analyze the weir annulus and drywell vent flows for reverse (containment to drywell) flow conditions. The analytical model and Clinton specific parameters were used to determine the weir annulus pool swell impact and drag velocities. Drag loads also were calculated for representative targets at selected elevations.

DEVELOPMENT OF ANALYTICAL MODEL

Shortly after a rupture in the primary system, the Emergency Core Cooling System (ECCS) pumps start automatically and pump condensate and/or suppression pool water into the reactor pressure vessel. This water floods the reactor core and then cascades into the drywell from the line break. It is assumed that the drywell is full of steam at this time, and that the sudden introduction of cool water causes rapid steam condensation and drywell depressurization. When the drywell pressure falls below the containment pressure, the drywell vacuum relief system is activated and air from the containment enters the drywell. Eventually, sufficient air returns to equalize the drywell and containment pressures. However, during this drywell depressurization transient, when there is a negative pressure from drywell to wetwell, reverse (inward) vent flow occurs. Then water can flow over the top of the weir wall into the drywell, and this is known as weir annulus pool swell ("weir swell").

The model is divided into two parts. The first part of this model describes the fluid reverse flow motion in the weir annulus and the vent system for reverse flow. The second part describes the fluid motion above the top of the weir wall.

Conservation of mass and energy were used to derive the equation of motion for weir annulus and vent flow. Figure 480.27-2-1 is a

sketch of the model used for this part of the analysis. One-dimensional, incompressible flow is assumed. Friction losses are assumed to be negligible, but the effects of irreversible entrance, exit and turning losses are included. The differential equation of motion obtained is:

$$\ddot{x} + \frac{\dot{x}}{2D(x)}\left[(1+B)\left(\frac{A_{WW}}{A_{DW}}\right)^2 - 1\right] + \frac{g}{D(x)}\left[\left(\frac{A_{WW}}{A_{DW}}\right)x + x\right] = g_c\frac{P(t)}{D(x)} \qquad \text{(Eq. 1)}$$

where:

x = the containment suppression pool water level,
$P(t)$ = containment pressure-drywell pressure,
B = the summation of the turning loss coefficients,
A_{WW} = containment suppression pool surface area,
A_{DW} = drywell suppression pool surface area,
A_V = drywell vent flow area,

$$D(x) = (z_2 - x) + \left(\frac{A_{WW}}{A_{DW}}\right)^2\left[z_1 + \left(\frac{A_{WW}}{A_{DW}}\right)x\right] + h\left(\frac{A_{WW}}{A_{DW}}\right)^2(k_5^2 + k_4^2) + \ell\left(\frac{A_{WW}}{A_V}\right)^2(k_2^2 + k_3^2 + k_4^2),$$

ℓ = the length of the horizontal vents,
h = the vertical distance between vent centerlines,
k_2 = fraction of total flow through top vent row,
k_3 = fraction of total flow through middle vent row,
k_4 = fraction of total flow through bottom vent row,
$k_5 = 1 - k_2$,
z_1 = the submergence of the top vent centerline, and
z_2 = the submergence of the bottom vent centerline

The fractions of the total flow through each vent (k_2, k_3, and k_4) were determined using the flow network shown in Figure 480.27-2-2. A set of three simultaneous non-linear alegebraic equations was obtained using this model. From the solution of these equations, it was determined that (k_2, k_3 and k_4) are independent of the drywell to wetwell pressure difference and are constant throughout the reverse vent flow transient. These parameters are used in determining the coefficient B and the function D(x) of Equation (1).

It was assumed that the water in the weir annulus is at the top vent centerline and that its upward velocity is negligible at the start of the transient. Equation (1) is valid as long as there is no flow over the top of the weir wall.

Once the weir annulus is full of water, the equation describing the fluid motion becomes:

$$\ddot{X} + \frac{\dot{x}^2}{2D(x)}\left[(1+B)\left(\frac{A_{ww}}{A_{DW}}\right)^2 - 1\right] +$$

$$\frac{g}{D(x)}\left(z_1' + x\right) = \frac{g_c}{D(x)}\, P(t) \qquad \text{(Eq. 2)}$$

where: z_1' is the distance from HWL to the top of the weir wall.

By substitution, the expression for D(x) becomes:

$$D(x) = \left(z_2 - x\right) + \left(\frac{A_{ww}}{A_{DW}}\right)\left(z_1 + z_1'\right) +$$

$$h\left(\frac{A_{ww}}{A_{DW}}\right)\left(K_5^2 + K_4^2\right) + \ell\left(\frac{A_{ww}}{A_v}\right)\left(k_2^2 + k_3^2 + k_4^2\right)$$

The initial conditions for this equation are obtained from Equation (1) at the time the water in the weir annulus reaches the top of the weir wall.

The wetwell to drywell pressure difference, P(t), was obtained by fit of a fifth order polynomial to the difference between wetwell and drywell pressure time histories during drywell depressurization. A least squares fit method was used to fit the polynomial to the discrete time pressure points.

Flow above the top of the weir wall is modeled as a free jet. The velocity potential, ϕ , and the non-steady state Bernoulli equation are used. For steady-state flow, the velocity, u, of the water at x_1 along the drywell wall (vertical flow) assuming inviscid flow is given by the center-line velocity of the free jet:

$$u = \left(\frac{-\partial \phi}{\partial x}\right)_{y=0} = \sqrt{V_o^2 - 2gx_1} \qquad \text{(Eq. 3)}$$

This expression is integrated with respect to x and differentiated with respect to time to obtain $\partial\phi/\partial t$. This partial derivative is substituted into the non-steady state Bernoulli equation. This equation is evaluated at $x_1 = 0$ where $u(o,t) = V_o(t)$ to determine the arbitrary function of time associated with the non-steady state Bernoulli equation. The resulting expression is:

$$u(x_1,t) = \left\{\left[V_o^2(t) - 2gx_1\right] + \frac{2V_o(t)\dot{V}_o(t)}{g}\left(V_o(t) - 2gx_1\right)^{1/2} - \frac{2V_o^2(t)\,\dot{V}_o(t)}{g}\right\}^{1/2} \qquad \text{(Eq. 4)}$$

where: x = height above the top of the weir wall.,

$V_o(t) = \frac{A_{ww}}{A_{Dw}} \dot{x}(t)$ = acceleration at the top of the weir wall, and

$\dot{x}(t)$ and $\ddot{x}(t)$ are obtained from Equation (2).

Equation (4) determines the center-line velocity of an unsteady free jet. Since at any height x_1, the center-line velocity is the maximum vertical component of the velocity, it is conservative to use Equation (4) for load calculation.

At the leading edge of the water slug ($x_1 = h$), the velocity is the impact velocity ($u = \dot{h}$). When these substitutions are incorporated into Equation (4), the differential equation for the impact velocity is:

$$\dot{h} = \left[(V_o^2 - 2gh) + \frac{2V_o\dot{V}_o}{g} (V_o^2 - 2gh)^{1/2} - \frac{2V_o\dot{V}_o}{g} \right]^{1/2} \quad \text{(Eq. 5)}$$

The initial condition for this equation is $h(t_o) = 0$.

Equation (4) is used to determine the drag velocity as a function of time at a given elevation. The value of x_1 is fixed for a given elevation in this equation. The acceleration was determined by numerically differentiating the drag velocity using a forward difference technique. The terms $V_o(t)$ and $\dot{V}_o(t)$ were obtained from Equation (2).

Equations (1), (2) and (5) were solved using the classical fourth order Runge-Kutta method. Equation (4) was solved at a fixed elevation.

Drag loads on a structure were estimated considering both the standard and inertia drag using the results from Equation (4). Impact pressures are determined using the methodology presented

in Table 480.27-2-2. The impact velocity used in determining impact pressure is obtained from Figure 480.27-2-5. Fallback drag loads are determined using Table 480.27-2-3.

ASSUMPTIONS AND INFORMATION

1. Clinton specific dimensions for the weir annulus and drywell vent system were used in the analyses.

2. Water flowing through the weir annulus and drywell wall vents is treated as one-dimensional, incompressible flow. However, since the water clears the weir wall, it is treated as an ideal (inviscid) fluid.

3. Friction is assumed to be negligible, but the effects of irreversible entrance, exit, and turning losses are included.

4. Evaluation of the reverse flow transient is initiated as the top vent row is recovered. It is assumed that the water in the weir annulus is at the top vent centerline and that its upward velocity is zero.

5. Containment suppression pool water level is allowed to decrease as water flows from the containment to the drywell. The analysis is terminated when the containment suppression pool water level drops below the bottom of the top vent row.

6. The velocity potential for the stream line adjacent to the drywell wall and the non-steady state Bernoulli equation are used to derive the impact velocity model.

7. Drywell to containment pressure difference time histories were incorporated by a least squares fit of a fifth order polynomial to the discrete pressures. The pressures obtained considering three of the four vacuum breakers opening was used. This case was used because it contains the maximum wetwell to drywell pressure difference.

8. The exit loss as the water clears the top of the weir wall and the pressure loss due to grating were included.

9. Actual location and dimensions of beams in the drywell were used to develop bounding load time histories.

10. The standard drag coefficient for grating was determined using Reference 5.

11. Standard drag and lift coefficients used in this calculation are presented in Table 480.27-2-3.

12. Inertia drag coefficients, C_m, were determined using the hydrodynamic masses obtained from Reference 6.

13. Pressure gradients within the weir swell jet in the vertical direction were assumed to be negligible.

RESULTS

Figure 480.27-2-3 is a plot of the wetwell to drywell pressure difference time history used in this calculation. This time history is for the case with three of four vacuum breakers operating. Both the fitted curve and the points used in determining this curve are plotted. The fitted curve has a standard deviation of approximately 0.026 from the data points.

Figure 480.27-2-4 is a plot of the velocity of the water in the weir annulus above the top vent centerline versus time. The water starts with an upward velocity of zero at the top vent centerline and reaches the top of the weir wall (dashed vertical line of Figure 480.27-2-4) at 1.87 seconds into the transient with a velocity of 8.7 feet per second. A maximum velocity of approximately 17.9 feet per second at the top of the weir wall, is reached by the end of the transient.

Impact velocity versus the height relative to the top of the weir wall (Elevation 735'9") is plotted in Figure 480.27-2-5. Structures located within the weir annulus above the top vent centerline and within 5 feet of the top of the weir wall will experience impact loading. A maximum impact velocity of approximately 9 feet per second occurs within the weir annulus but diminishes to $\leq$ 1 foot per second within 2 feet above the top of the weir wall.

Figure 480.27-2-6 is a plot of the drag load time histories for a 10-inch diameter pipe (10.75-inch O.D.) at selected elevations. Both standard and inertia drag are included. Drag loads are presented per foot of pipe. A maximum load of approximately 384 pounds per foot is calculated for 10-inch diameter pipes located within the weir annulus.

The drag load time history, for the grating at Elevation 737'0" shown in Figure 480.27-2-7, is per square foot of gross grating area. A maximum load of approximately 120 pounds per square foot occurs. Figure 480.27-2-8 is a plot of the drag load time histories for representative beams used to support the grating. These loads are presented per foot of beam length. These loads apply only to the section of the beam above the weir annulus. As shown in Figure 480.27-2-8 maximum drag loads of 281 to 890 pounds per foot are a function of the size of the beam.

Weir swell impact loads are to be calculated using the methodology presented in Table 480.27-2-2 (per Reference 4). Plant specific impact velocities from Figure 480.27-2-5 are used with this methodology to evaluate plant specific impact loads.

The impact velocity at the lower edge of the structure was used. The impact duration, τ , is dependent on the structure's orientation as described in Table 480.27-2-2. It should be noted that per Reference 4, grating does not experience an impact load.

Structures located within the drywell also will experience fallback drag loads calculated using the methodology presented in Table 480.27-2-3. Per Reference 4, impact loads are not applicable during fallback. The zones of influence for weir swell impact and fallback loads are shown on Figure 480.27-2-9. Per Reference 8, the upper bounding streamline is represented by a cycloid. The closest approach of the falling water to the edge of the RPV biological shielding wall is approximately 12 feet. The coordinates describing the upper swell boundary are listed in Table 480.27-2-4.

Weir swell impact loads may be applied as static or dynamic loads. When these loads are applied as static loads appropriate dynamic load factors are used.* The impact and drag loads were evaluated separately and the responses combined using an appropriate method to obtain a response envelope. For a dynamic analysis, the impact load history was superimposed on the drag load time history. The resulting load envelope was applied to the structure under investigation.

The loads presented in Figure 480.27-2-6 may be scaled to conservatively approximate the loads on smaller diameter pipes and conduits (less than 10.75 inches), may be approximated by multiplying them by the ratio of the pipe or conduit diameter to 10.75 inches. It is not appropriate to use this ratio to scale loads when the conduit is within one diameter of a boundary or an adjacent structure (conduit, pipe, beam, etc.) where this structure can interfere with the flow field and substantially change the drag coefficients.

Results of these calculations show that structures located in the weir annulus above the top vent centerline and within 5 feet above the top of the weir wall are affected by weir swell. Significant impact and drag loads result from this phenomenon.

---

* As an example, see Reference 4, Figure 3B.30(c)-2

COMPARISON WITH GESSAR-II

A comparison of GESSAR-II and Clinton geometrical parameters in Table 480.27-2-5, reveals the following:

- The Clinton suppression pool volume is ~15% larger than the GESSAR standard 238 plant.

- The vent systems are similar except in the number of vents. Clinton's vent flow area is ~85% of the standard plant flow area.

- The weir wall in the standard plant is some 2.3 feet higher than the weir wall for Clinton.

- The weir annulus area to vent area ratio is less than 1.0 for the standard plant and greater than 1.0 for the Clinton plant.

In terms of the weir swell modeling, the larger suppression pool volume effect is to prolong the transient. Likewise, the effect of a lesser number of vents is to reduce the rate of water flow into the containment and thus extend the transient. The effect of the extended duration is to more closely approach the steady state maximum theoretical drag velocity.

The effect of the lower weir wall at Clinton is to decrease the acceleration of the water as it passes through the vent/weir system and for a given pressure differential, produce less acceleration and lower velocities.

The effect of the weir annulus area to vent area ratio is to effect a lower acceleration, thus a lower velocity at Clinton.

Table 480.27-2-5 also contrasts pertinent assumptions used in the two solutions. The most significant difference is in the differential pressure assumptions. The standard plant assumption

of a constant pressure differential and the steady state solution leads to determination of only the maximum drag velocity. The attendant time-history information must be assumed in order to properly design the affected structures. The Clinton assumption of a pressure differential time-history properly accounts for the dynamics throughout the transient and leads to a more realistic time history shape. The steady state drag velocity is as shown in Figure 480.27-2-4. A further benefit of this assumption is that the proper timing between the impact and drag loads is established, thus eliminating the need to combine the maximum of the two loads in an overly conservative manner.

The effect of the standard plant assumption related to the hydrostatic head is to overstate the driving pressure differential and thus the maximum drag velocity. The Clinton assumption properly accounts for the lower driving pressure which results from the suppression pool flowing into the vent/weir system.

Since the standard plant solution is only directed toward the maximum values, the initial water level assumptions are of no consequence. However, the steady assumptions would underestimate the velocities in the early portion of a time history if it were produced. The Clinton assumption, zero velocity at the top vent centerline, is conservative with respect to the expected condition, zero velocity at the top of the top vent. This assumption maximizes the acceleration and thus the impact velocity during the early stages of the transient.

The friction loss assumptions affect primarily the maximum values of the velocities. They also have a minor effect on the shape of the time-history. The GESSAR-II assumptions were chosen to assure that the maximum drag velocity was determined for application to a wide range of situations. The Clinton assumptions are believed appropriate for the Clinton plant.

The pertinent results are the maximum velocities and the maximum height of the weir swell phenomenon. The thrust of the GESSAR-II analysis was to produce a conservative upper bound for these parameters. This emphasis is reflected in the 30 feet per second drag velocity and the 14 foot weir swell height. The more realistic modeling for the Clinton plant results in a maximum drag velocity of 18 feet per second and 5 foot weir swell height. The effects of the larger suppression pool and higher maximum pressure differential are offset by the effect of friction and the time-history analyses.

The maximum impact velocity is determined during the initial acceleration of the water slug in the weir annulus. The peak value is reached prior to the water filling the weir annulus. Thus, the highest impact velocities are limited to the weir annulus.

The GESSAR-II model has not considered the flow in the weir annulus for impact loads. Thus comparison between the two models is not possible for this flow regime.

REFERENCES

1. NSLD Calc. No. 3C10-0976-002, Rev. 0, "Maximum External Drywell Pressure on the Drywell Structure", November 29, 1976, (Approved).

2. I. E. Idel'Chik, Handbook of Hydraulic Resistance, Coefficients of Local Resistance and of Friction, 1960.

3. Univac, Large Scale Systems Math-Pack Programmers Reference, 1970.

4. Appendix 3B to GESSAR-II 238 Nuclear Island, G. E. Document 22A7000, Rev. 2, dated June 15, 1981.

5. S. F. Hoerner, Fluid-Dynamic Drag, 1958.

REFERENCES (Cont'd)

6. K. T. Patton, "Tables of Hydrodynamic Mass Factors for Tranlational Motion", 1965.

7. Interoffice Memorandum from J. M. Park to W. R. Peebles, "Cross-sectional Properties/Dimensions of Structural Steel at Top of Weir Wall", October 27, 1981.

8. Milne-Thomson, Theoretical Hydrodynamics, pp. 303-305, fourth edition, MacMillian & Co., New York (1960).

TABLE 480.27-2-1

FIGURE 480.27-2-2 NETWORK EXPLANATION

Node Number	Description
1	Pressure due to top vent submergence
2	Pressure due to middle vent submergence
3	Pressure due to bottom vent submergence
4	Loss at entrance
5	Friction loss (1)
6	Loss at tee junction
7	Loss at entrance
8	Friction loss (1)
9	Loss at tee junction
10	Loss at entrance
11	Friction loss (1)
12	Loss at tee junction
13	Pressure loss due to elevation difference between bottom and middle vents
14	Friction loss (1)
15	Loss in tee junction
16	Pressure loss due to elevation difference between middle and top vents
17	Friction loss (1)
18	Loss in tee junction
19	Pressure loss due to elevation difference between top vent and top of weir wall
20	Friction loss (1)
21	Loss at exit and pressure loss due to grating

(1) Friction losses are assumed to be zero.

TABLE 480.27-2-2*

IMPACT METHODOLOGY SUMMARY

1. Determine the impulse per unit of target area from the correlations given below. The impulse is given by an expression of the form

$$I = \alpha V/32.2$$

where:

I = impulse per unit area (1bf-sec/ft^2)
V = plant-unique transient jet front velocity at structure location (see Figure 480.27-2-5)
and α depends on the target geometry as follows:

Cylindrical target	$\alpha = 0.81\ D$
Flat target	$\alpha = 2.5\ W$

with
D = target diameter (in)
W = target width (in)

2. An impulse duration of 2 msec for circumferential targets and 6.8 msec for radial targets can be used per Reference 4.

3. Compute peak pressure from:

$$P_{max} = \frac{2I}{144}$$

where: P_{max} = peak pressure (psi)

τ = impulse duration (sec.)

TABLE 480.27-2-2* (Cont'd)

4. The impact pressure time history has the form:

$$P(t) = 0.5P_{max} \ (1-\cos 2\pi t/\tau) \ (psi).$$

---

* per Reference 4, Table 3B.30(c)-1

TABLE 480.27-2-3

WEIR ANNULUS POOL SWELL FALLBACK DRAG LOAD

$$F_V = \frac{C_D \rho D V}{2 g_c} + \frac{C_H g A_s \rho}{g_c} = \text{vertical component load, } (lb_f/ft)^1$$

where ρ = density of water (62.4 lb_m/ft^3)

g_c = gravitation acceleration constant, (32.2 ft-lb_m/sec-lb_f)

D = diameter of pipe or width of beam, (ft)

V = freefall drag velocity, (ft/sec)

C_D = standard drag coefficient

= 1.2 for pipes with no interference effect

= 2.0 for flat surfaces with no interference effect

C_H = hydrodynamic mass coefficient

= 1.0 for pipes with no interference effect

= 9.7 for W12x85 beams with no interference effect

= 7.2 for W12x120 beams with no interference effect

= 5.0 for W14x370 beams with no interference effect

= 4.9 for 1CG10 and 1CG11 beams with no interference effect

g = acceleration due to gravity, (32.2 ft/s^2)

A_s = cross sectional area of loaded structure, (ft^2)

---

(1) Vertical loads are to be applied as a step function with a duration of 11.75 seconds.

(2) A duration of 11.75 seconds should be used.

TABLE 480.27-2-3 (Cont'd)

$$V = \sqrt{2x32.2(740.76 - y)} \text{ (ft/sec)}$$

y = the elevation under consideration, (ft)

TABLE 480.27-2-4

UPPER WEIR SWELL BOUNDARY

Radius from RPV Centerline (ft)	Elevation (ft)
26.59	735.75
26.61	735.90
26.73	736.34
27.05	737.01
27.63	737.83
28.51	738.71
29.68	739.53
31.12	740.20
32.76	740.63
34.50	740.75

TABLE 480.27-2-5

COMPARISON OF WEIR SWELL PARAMETERS

PARAMETER	GESSAR-II	CLINTON
ID	83'0"	79'0"
OD	120'0"	124'0"
High/Normal Water Level	20'5"	19'5"
Area in Wetwell	5900 ft^2	7175 ft^2
Horizontal vents		
- number	120	102
- diameter	27.5"	27.5"
- submergence T/C/B@NWL/HWL	7'6"/12'0"/16'5"	7'6"/12'0"/16'5"
- total flow area	495 ft^2	420 ft^2
Weir wall height	26'1"	23'9"
Area in drywell	482 ft^2	455 ft^2
Modeling Assumptions		
Driving Wetwell/Drywell Pressure differential	14.0 psid constant	0-15.7 psid time-history
Static head of Suppression pool	constant based on HWL	variable based on time dependent water level.
Initial conditions	zero velocity at top of weir wall	zero velocity at of top vent
Friction losses	none (exit loss for weir wall)	entrance, exit losses, grating losses.

TABLE 480.27-2-5 (Cont'd)

Results

Maximum drag velocity	30 ft/sec	18 ft/sec
Maximum impact velocity	10 ft/sec	9 ft/sec*
Maximum swell height (above top of weir wall)	14 ft	5 ft**

* Maximum impact velocity occurs in the weir annulus (3' from top of wall)

** Velocity is zero at this level.

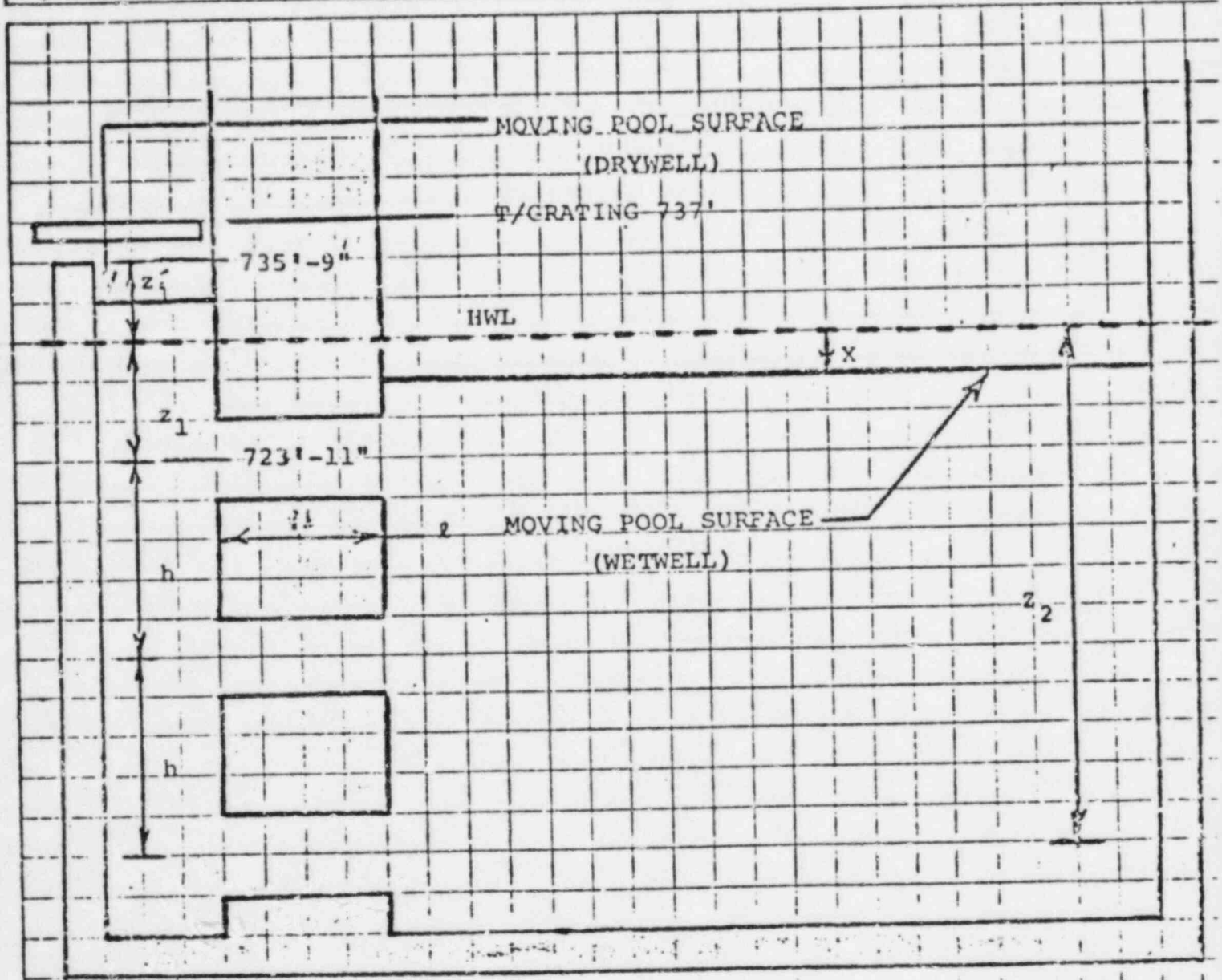

Figure 480.27-2-1

FIGURE 1: Reverse Vent Flow Model

Figure 480.27-2-2

FIGURE 2

FLOW NETWORK

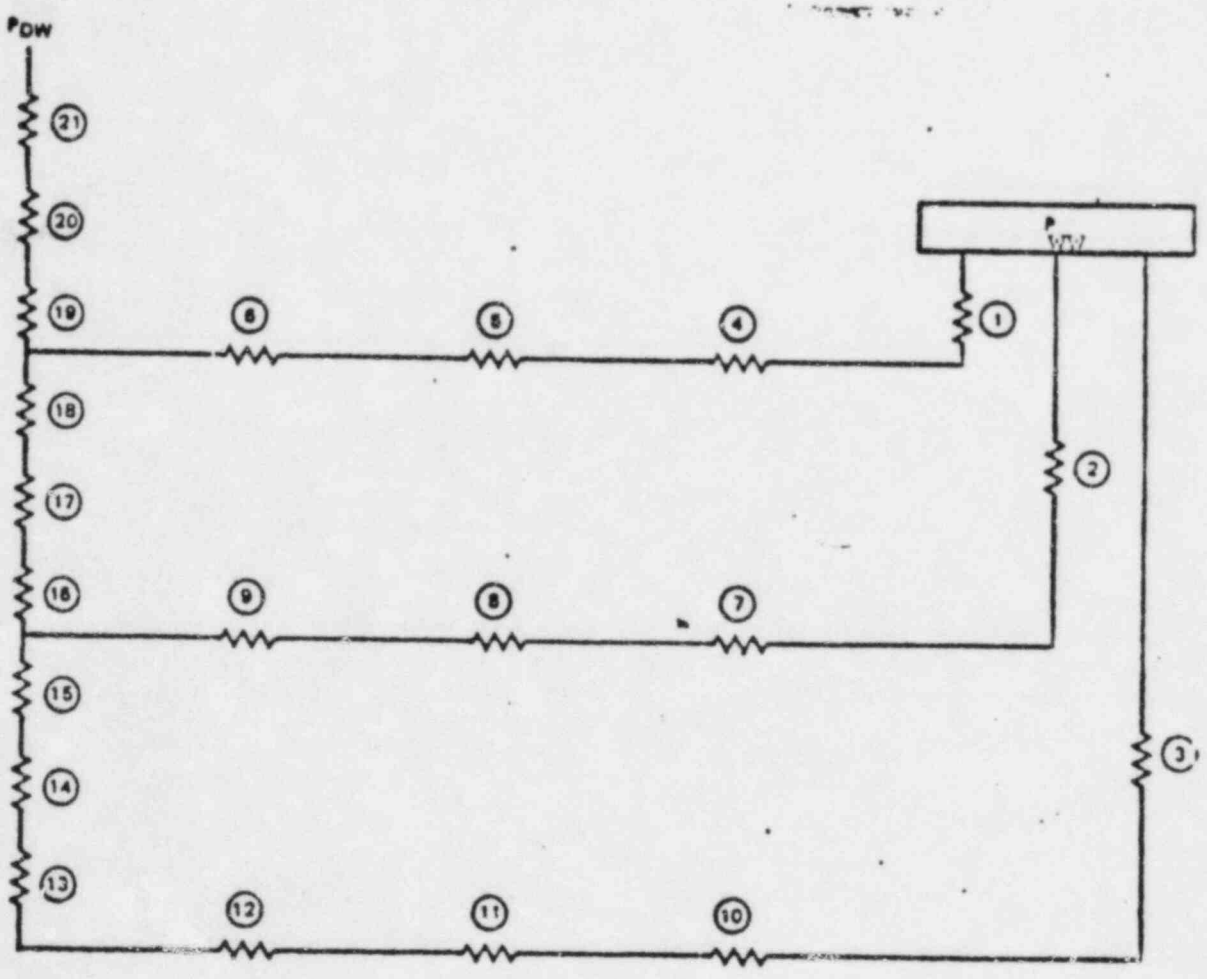

Note: See Table 1 for network explanation.

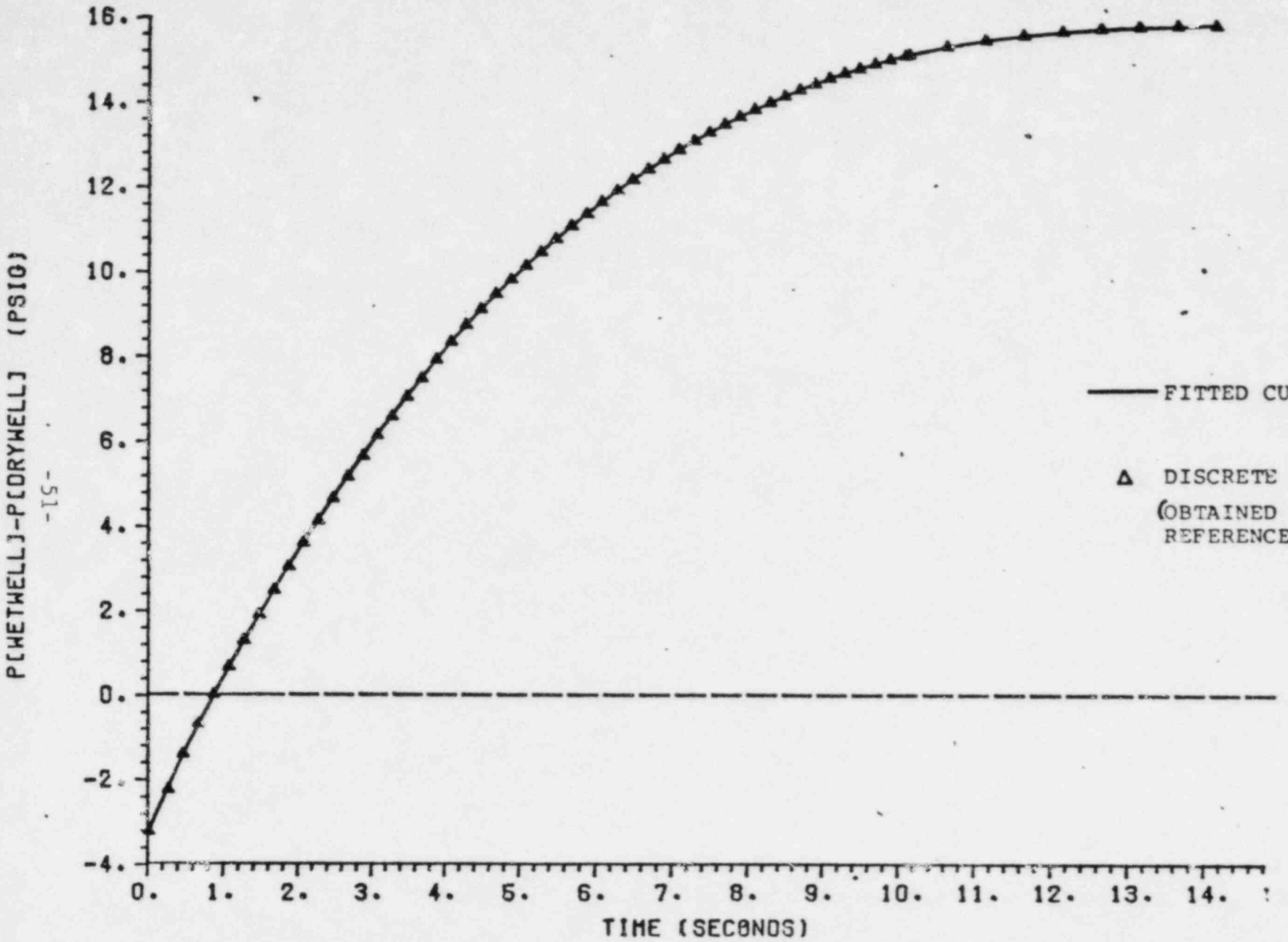

Figure 480.27-2.3

FIGURE 3: WETWELL TO DRYWELL PRESSURE DIFFERENCE - 3 VB OP

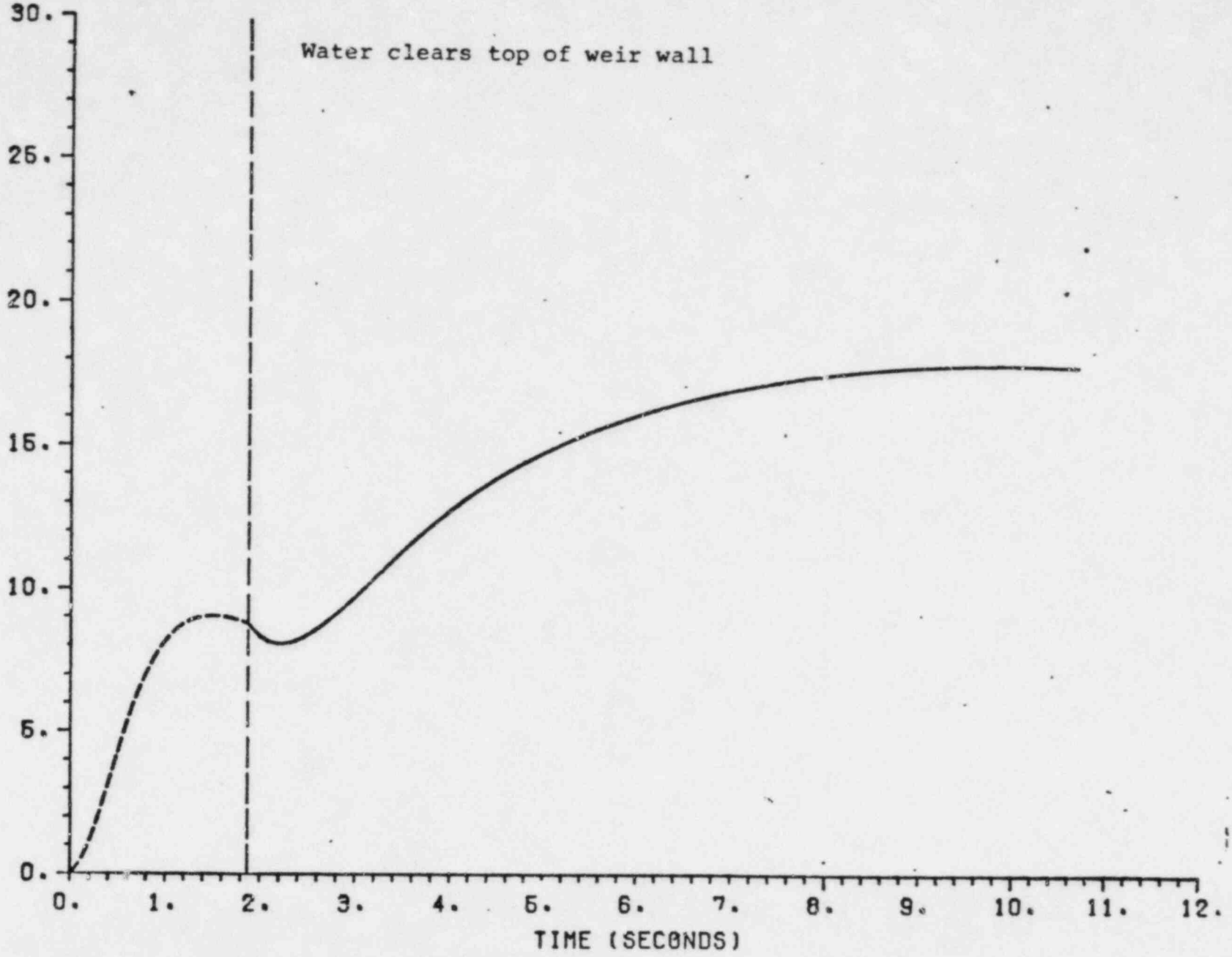

FIGURE 4: WATER VELOCITY IN WEIR ANNULUS

Figure 480.27-2-4

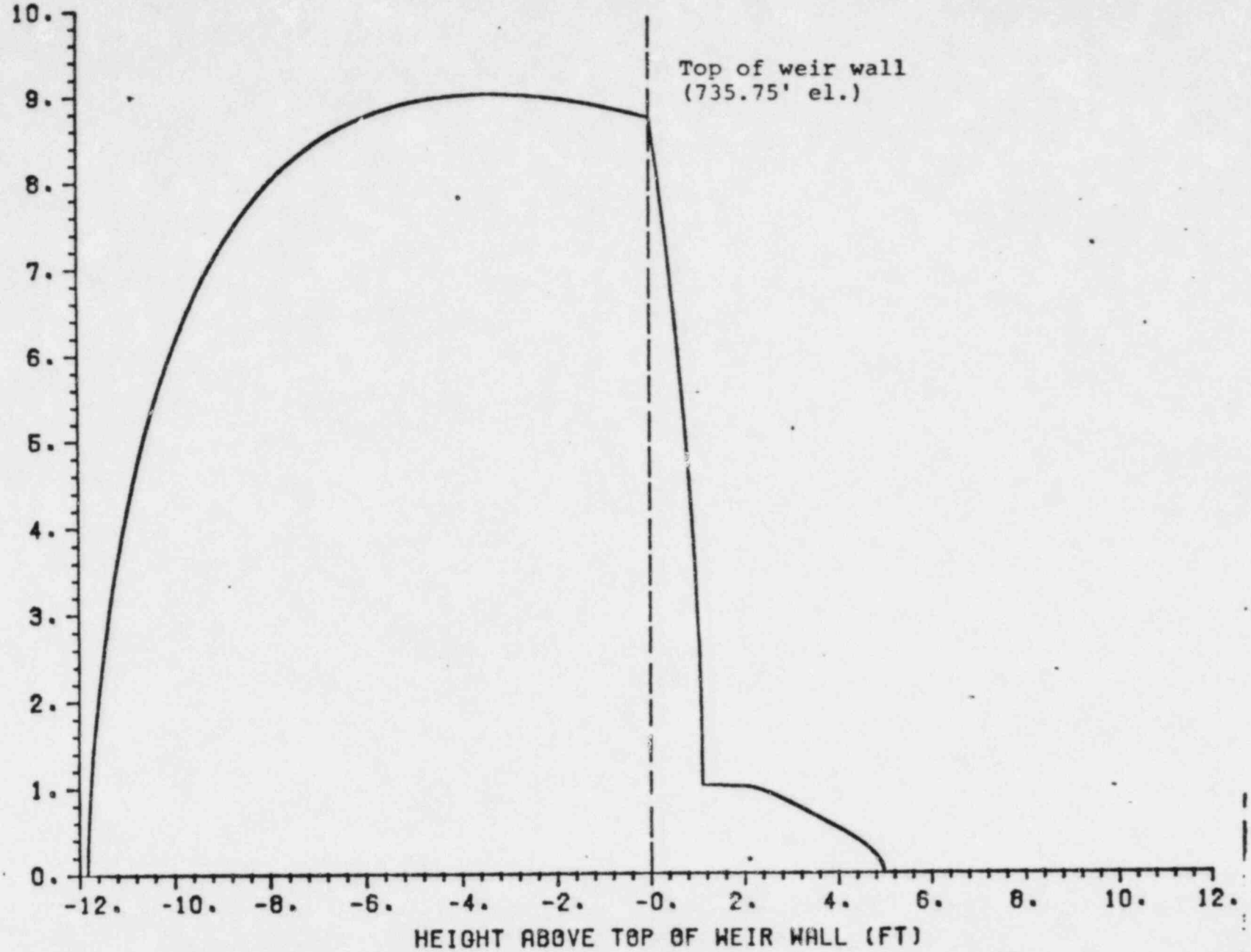

FIGURE 5: IMPACT VELOCITY VS. HT. ABOVE TOP OF WEIR WALL

Figure 480.27-2-5

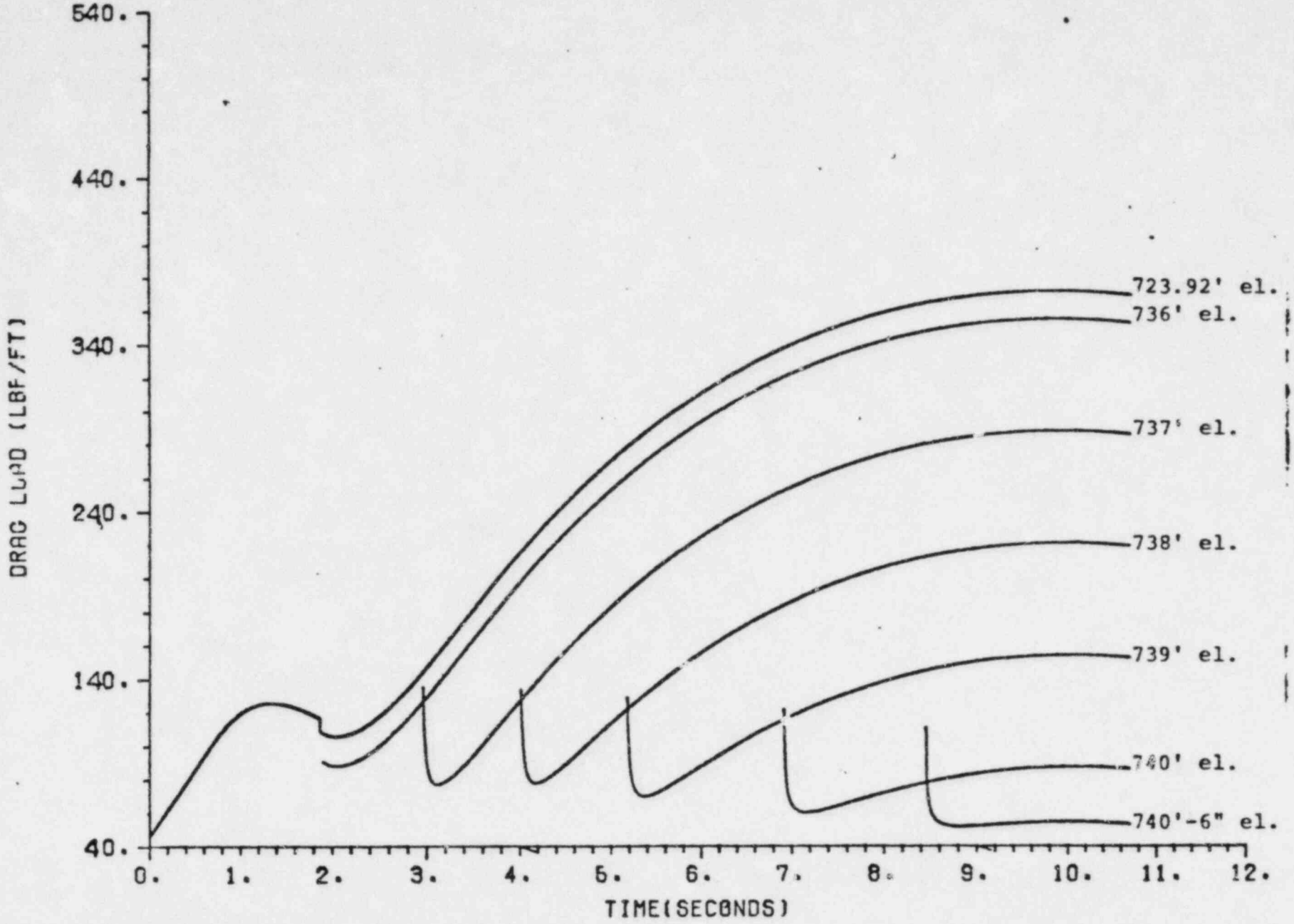

Figure 480.27-2-6

FIGURE 6: WEIR ANNULUS POOL SWELL DRAG LOADS ON 10" HORIZONTAL PIPE

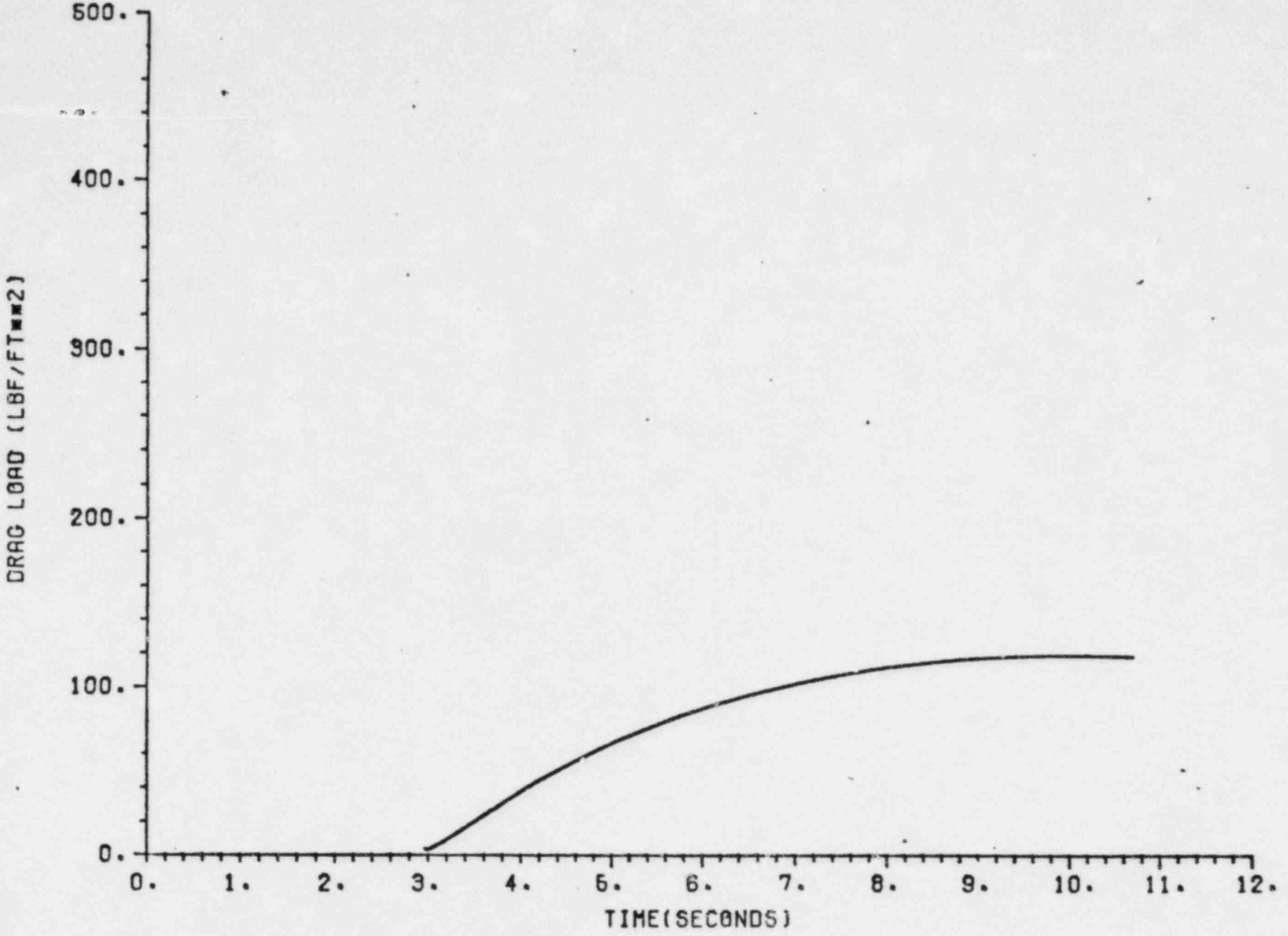

Figure 480.27-2-7

FIGURE 7: WEIR ANNULUS POOL SWELL DRAG LOADS ON GRATING - 737 FT. EL.

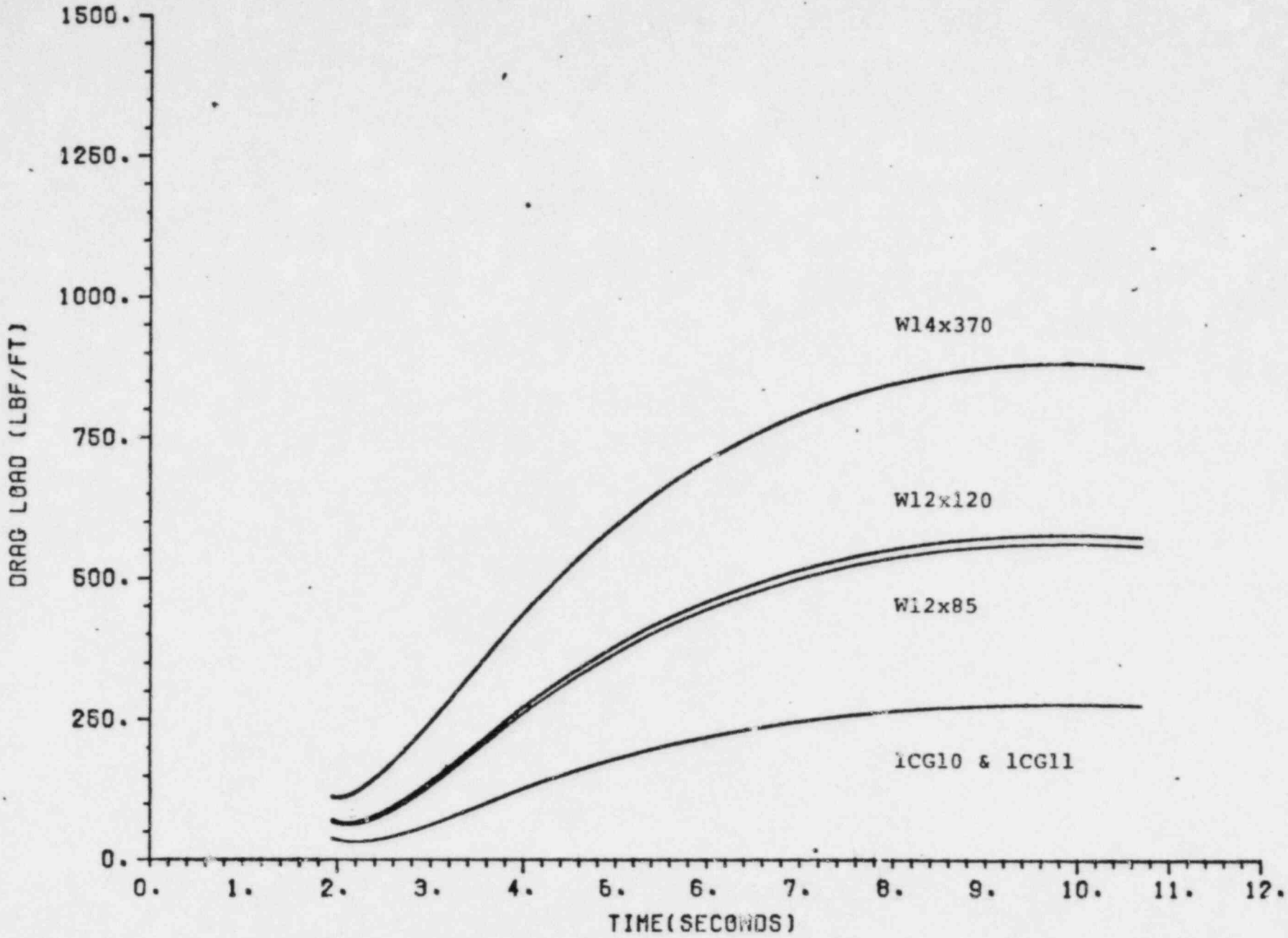

Figure 480.27-2-8

FIGURE 8: WEIR ANNULUS POOL SWELL DRAG LOADS ON I BEAMS

Figure 480.27-2-9

Figure 9

Weir Annulus Pool Swell Zone of Application

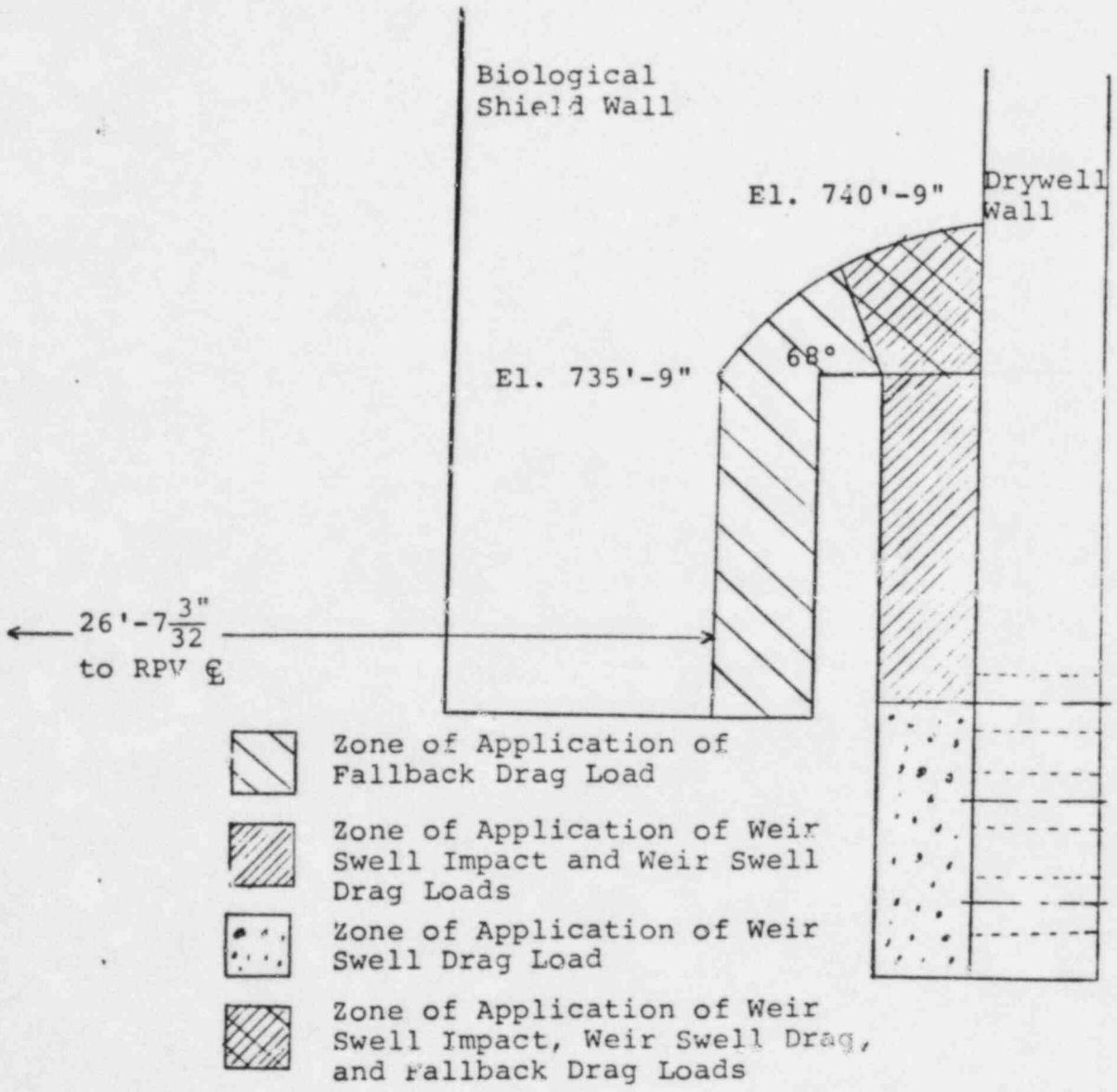

NRC QUESTION NO. 480.27

In order to demonstrate the adequacy of the Clinton containment design regarding LOCA related hydrodynamic loads, the following information needs to be supplied for our review.

3) Provide and justify any modifications made to the generic load definition for the Clinton Confirmatory Analysis.

RESPONSE

In addition to the loads discussed in the response to Question 480.27-2, the two phase flow P load acting across the MCU floor has been calculated using Clinton unique parameters. These calculations showed that P for Clinton would be 4.6 psi instead of 11 psi given in the GESSAR. The calculations were based on an open area of greater than 26% of the floor.

REQUEST 480.28

In order to conform to the criteria of NUREG-0783, the applicant should confirm that a single failure analysis has been performed in the system design and power source to demonstrate that the loss of the RHR heat exchangers and the RHR shutdown cooling mode will not occur.

RESPONSE:

To meet the requirements of General Design Criterion 34 and as indicated in CPS FSAR Appendix 15A, a single failure analysis has been done on the shutdown cooling system of the RHR system (Reference Article 15A.6.3.3, event 18, and Figure 15A.6-18 which addresses shutdown cooling specifically).

In the unlikely event that offsite power is lost, and assuming the worst-case failure to be the loss of one division of emergency power, actuation of one of the shutdown cooling line valves to the open position would be prevented. In the postulated single failure described above, the single shutdown suction line will be unable to draw water from the vessel for the cooldown operation.

Given the unlikely condition that suction line isolation loss occurred and could not be corrected by operator actions, alternate shutdown cooling would be achieved using redundant safety grade equipment.